Brightness Fields of Broken Clouds

V. E. Zuev, G. A. Titov, E. I. Kasyanov, and D. A. Zimin
Institute of Atmospheric Optics, Siberian Branch
Russian Academy of Sciences
Tomsk, Russia

Introduction

The radiation budget and brightness field of the system "atmosphere-underlying surface" are controlled, to a considerable degree, by the variety of forms and the strong space-time variability of cloud cover. The space and angle structure of the radiation fields of cloudy atmosphere together with their sensitivity to cloud variations provide an important source of information needed to formulate and solve problems of the remote optical sensing of cloudy atmosphere (e.g., King 1987; Yi et al. 1990) and of satellite meteorology, as well as for retrievals of the albedo from satellite measurements (Green 1980; King and Curran 1980).

Recent theoretical studies are largely based on the solution of the equation of radiative transfer in a plane-parallel, horizontally homogeneous cloud layer partially or completely covering the sky. However, such a simple model overlooks significant effects associated with the random geometry of the cloud field and, in fact, the important role it plays in the formation of the radiation budget and brightness fields of the cloudy atmosphere. The presence of the above limitations, as well as a variety of related unsolved problems, for instance, with the interpretation of satellite data (Gabriel et al. 1988), has recently stimulated the development of the radiative transfer theory in stochastic scattering media (see, for example, Barker and Davies 1992; Davis et al. 1990, 1991a, 1991b; Gabriel et al. 1990; Pomraning 1991a, 1991b; Stephens 1988a, 1988b; Titov 1990; Zhuravleva and Titov 1987, 1989a, 1989b).

Model of the Atmosphere and Method of Solution

We restrict ourselves to the treatment of an atmospheric model consisting of three layers: cloudy (Λ), above- (Λ_2),

and under-cloud (Λ_1) aerosol layers over a lambertianly reflecting underlying surface with an albedo A_s.

The above- and under-cloud aerosol layers are considered to be horizontally homogeneous, with the optical thicknesses $\tau_{a,1}$ and $\tau_{a,2}$; single scattering albedos λ_1, and λ_2; and a common, altitude-independent scattering phase function. The optical characteristics of the above- and under-cloud aerosol layers correspond to those from the background model of continental aerosol (*Atmosphere Handbook* 1991). The scattering phase function used is for the Haze *L* model and for the wavelength 0.69 µm (Deirmendjian 1969). Above 20 km, the aerosol and molecular scattering coefficients vanish and are, thus, neglected.

The statistically homogeneous and nonisotropic cloud field is generated by the Poisson point fluxes (Titov 1985, 1990). In addition to traditional parameters, also used as model input are the cloud fraction, *N*, and the mean (characteristic) horizontal cloud size, *D*, which determines the correlation function of cloud field. If in clouds, we compute with the scattering phase function for the C_1 cloud (Deirmendjian 1969), calculated from the Mie theory for the 0.69 µm wavelength.

Mean and variance of the specific intensity of reflected solar radiation were computed using the Monte Carlo method algorithms developed based on the equations for the mean and correlation function of specific intensity (Zhuravleva and Titov 1989a, 1989b; Titov 1990).

Numerical Results

Suppose the atmospheric top is illuminated by the unit, parallel flux of solar radiation. The solar incidence is defined by the zenith, $\xi_\otimes$, and azimuthal, $\varphi_\otimes$, angles, with the latter set as zero throughout the computation. The receiver has the field of view angle $\alpha = 10^{-3}$ *rad*, and its optical axis orientation in space is defined by the zenith, θ,

and azimuthal, φ, angles. The absolute values can be obtained by multiplying the numerical results by $S_\lambda \cos\xi_\otimes$, with S_λ the spectral solar constant.

The statistical characteristics of visible solar radiation were computed simultaneously for the set of zenith $\theta = 0,10,20,30,40,50,60,70,80°$ and azimuthal $\varphi=0,30,60, 90,120,150,180°$ angles, as well as for the values of surface albedo $A_s = 0,0.2,0.4,0,6,0.8,0.9$. These last values cover the entire range of earth's surface albedo (from ocean to new-fallen snow). Since the radiation field is symmetrical about the plane of solar vertical, we can restrict our consideration to the range $0 \leq \varphi \leq 180°$. The relative computation error was within 1% to 5% for most of the calculations.

The mean intensity of reflected solar radiation as modulated by cumulus ($£I_{Cu}ß$) and equivalent stratus ($£I_{St}ß$) clouds is given in Figure 1. Here and below, by equivalence we mean the following: cumulus and stratus cloud fields have the same optical and geometrical characteristics, but differ in the parameter $\gamma =: H/D$ (H is the cloud layer thickness) whose value is approximately 1 for cumulus and does not exceed $10^{-2} - 10^{-3}$ for stratus (*Handbook of Clouds and Cloudy Atmosphere* 1989). Such a cloud field is statistically homogeneous and nonisotropic, and the cloud bases are, on the average, squares. The latter fact implies that in the *XOY* plane, the cloud optical characteristics, on the average, possess the mirror symmetry about a straight line that passes through an arbitrary point and forms with the vertical the angles $\varphi = 0, \pm45, 90°$. Obviously, at $\xi_\otimes = 0°$, $£I_{Cu}ß$ itself must possess, on the average, the same symmetry. This statement is supported graphically by Figure 1a. For horizontally homogeneous stratus clouds under overhead sun, $£I_{St}ß$ is invariant to the azimuthal viewing angle φ (Figure 1b); slight variations with φ are caused by the computation error. Notice that $£I_{St}ß$ is maximum for a nearly zero zenith viewing angle and decreases as θ grows; for cumulus, the reverse is true. Qualitatively, this means that $£I_{St}ß$ and $£I_{Cu}ß$ may behave differently with θ.

Further, the radiation field is strongly dependent upon the solar zenith angle. At larger $\xi_\otimes$, the anisotropy of radiative field is more pronounced. Despite the fact that the underlying surface reflects lambertianly, this anisotropy persists even for large A_s, and the brightness fields of cumulus and stratus clouds can be significantly different (Figure 2). Dependence upon the spatial orientation of the receiver is

strongest for $\theta > 50° - 60°$ and $\varphi < 90°$, in which case the mean intensity varies several-fold. This dependence is easily explained by considering the strong forward elongation of the scattering phase function of clouds and the solar zenith angle prescribed. For nearly overhead sun, the mean fluxes of direct radiation are almost insensitive to the cloud type. Owing to the strong forward peak of the scattering phase function, radiation exiting through the sides of cumulus clouds represents a major contributor to the transmission; thus, for reflected radiation, the inequality $£I_{Cu}ß < £I_{St}ß$ holds almost over the entire range of zenith viewing angles θ (for the given problem parameters, this occurs for $\theta < 60°$) (Figure 1). At large $\xi_\otimes$ incident solar radiation is attenuated by the sides of cumulus clouds; therefore, the mean unscattered radiation fluxes in cumulus can be significantly less than in equivalent stratus, while for diffuse fluxes, the opposite is true. For this reason, at $\xi_\otimes = 60°$ the inequality $£I_{Cu}ß > £I_{St}ß$ can be valid (Figure 2).

The mean intensity $£I_{St}ß$ is a linear function of cloud fraction, i.e., $£I_{St}ß$ varies with *N* independently of θ (Figures 3a and 3b). In the cumulus cloud case, $£I_{Cu}ß$ depends nonlinearly on *N*, and the character of this dependence is extremely sensitive to θ. The mean intensity $£I_{Cu}ß$ is most sensitive to cloud fraction at small *N* and large θ, in which case the partial derivative $\partial£I_{Cu}ß/\partial N$ is maximum. For the stratus clouds, the variance D_{St} is symmetrical about $N = 0.5$, and the magnitude of its maximum is a strong function of viewing angle (Figures 3c and 3d). The intensity variance in cumulus, D_{Cu}, is significantly less than D_{St}, the variance in stratus. This is attributable to the fact that, given any sampling realization of the cumulus cloud field, a finite field-of-view receiver records not only radiation coming from cloud tops, but also that from the sides of individual clouds. As a result, the cloud field fluctuations will be smoothed out, on the average. At small θ, the maximum of D_{Cu} locates in the vicinity of N ~ 0.5 and shifts, with increasing θ, toward smaller cloud fractions. This shift of the D_{Cu} peak is attributable to the fact that the influence of cumulus cloud sides on the radiative transfer is also dependent upon the viewing angle.

Radiation reflected from the surface can be scattered by clouds, and its considerable portion is then reflected backward to the surface. In addition, some portion of this radiation propagates in the cloud gaps ("holes"), and since the aerosol atmosphere is optically thin, this radiation may contribute significantly to the brightness field of solar
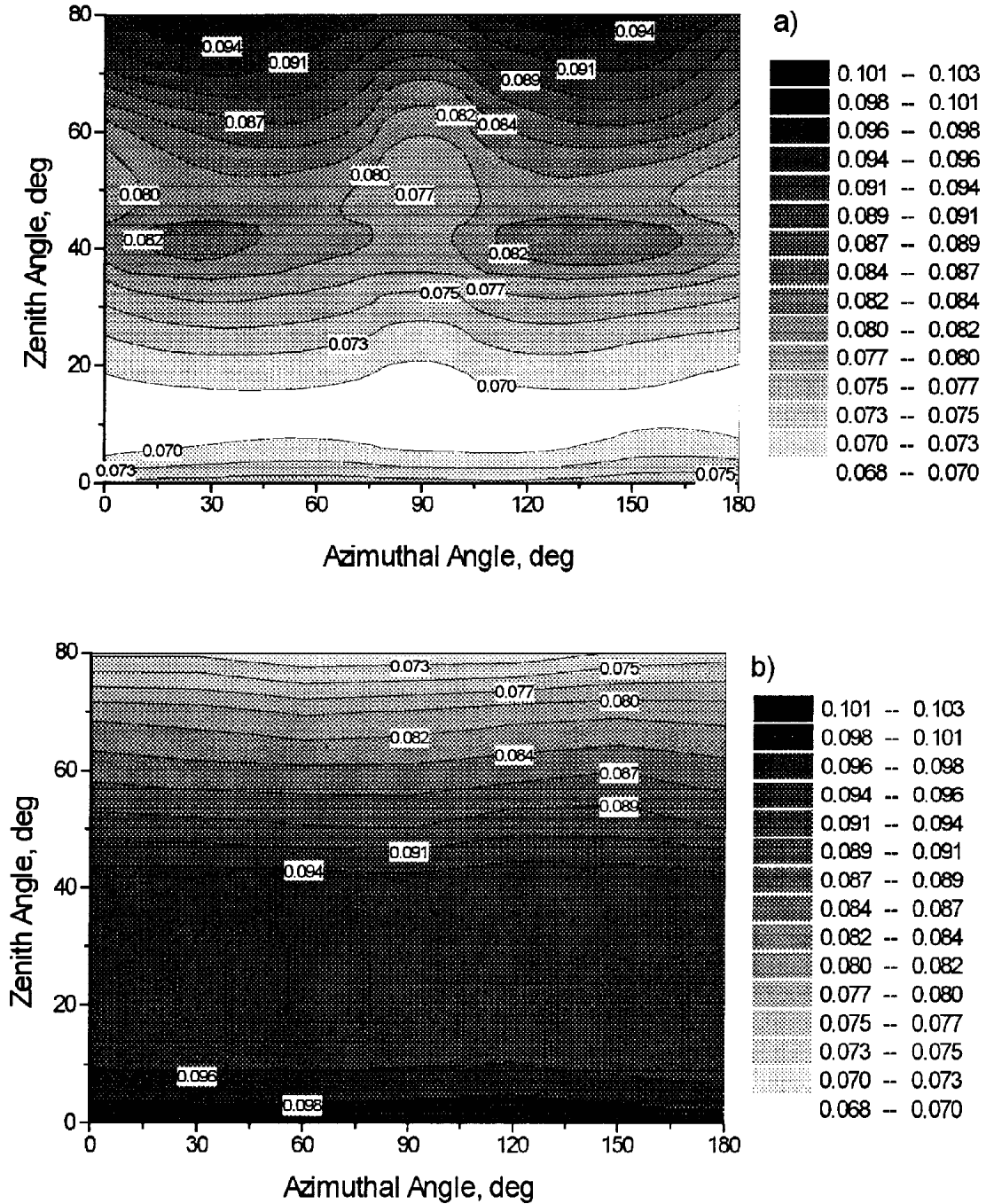
Figure 1. Mean intensity of reflected solar radiation with $\xi_\otimes = 0°$, $N = 0.5$, $\sigma = 30$ km^{-1}, $H = 0.5$ km, $A_s = 0$; (a) cumulus clouds (γ=1), (b) stratus clouds (γ=0).
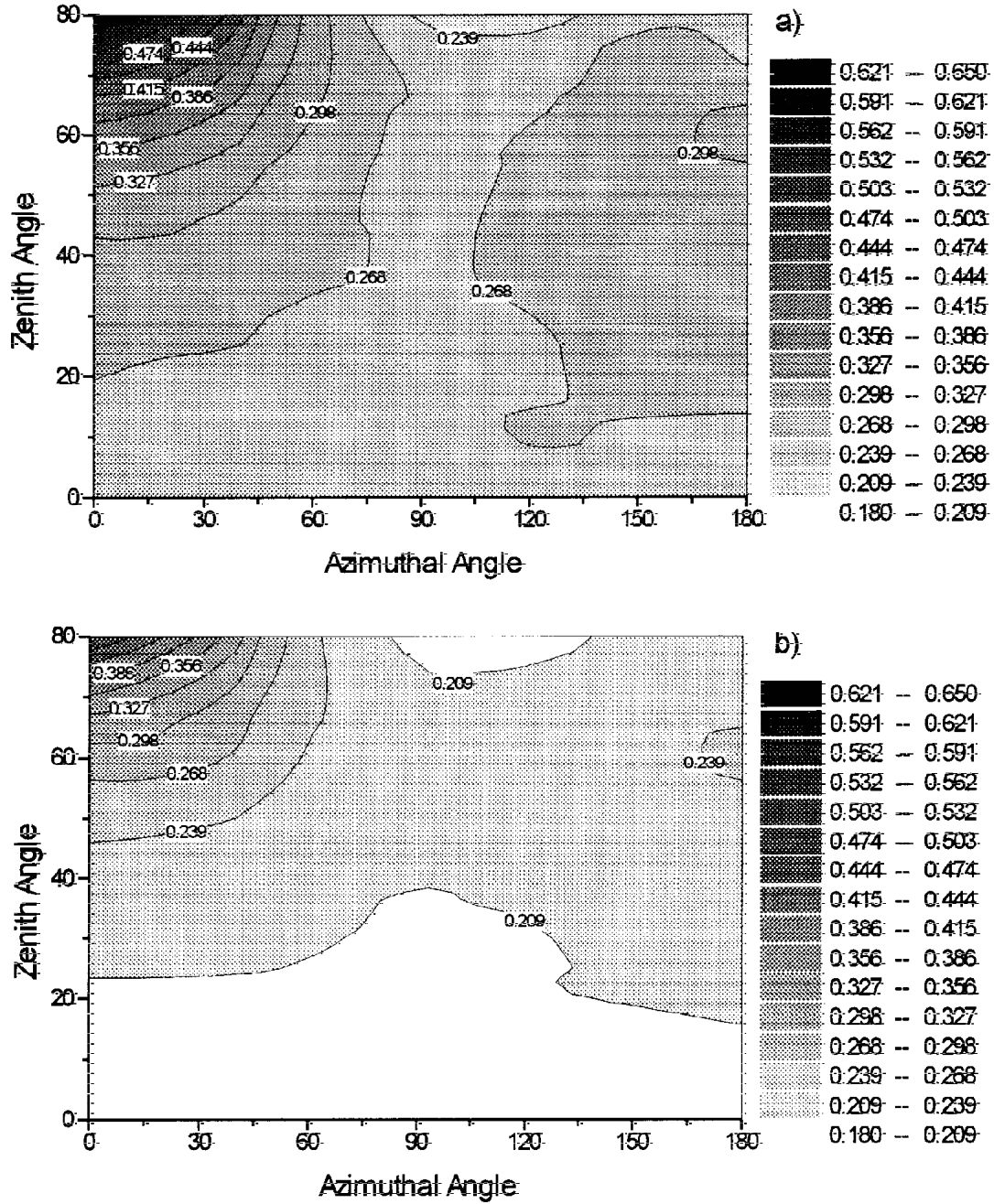
Figure 2. Mean intensity of reflected solar radiation with $\xi_{\otimes} = 60°$, $N = 0.5$, $\sigma = 30$ km^{-1}, $H = 0.5$ km, $A_s = 0.9$; (a) cumulus clouds ($\gamma=1$), (b) stratus clouds ($\gamma=0$).
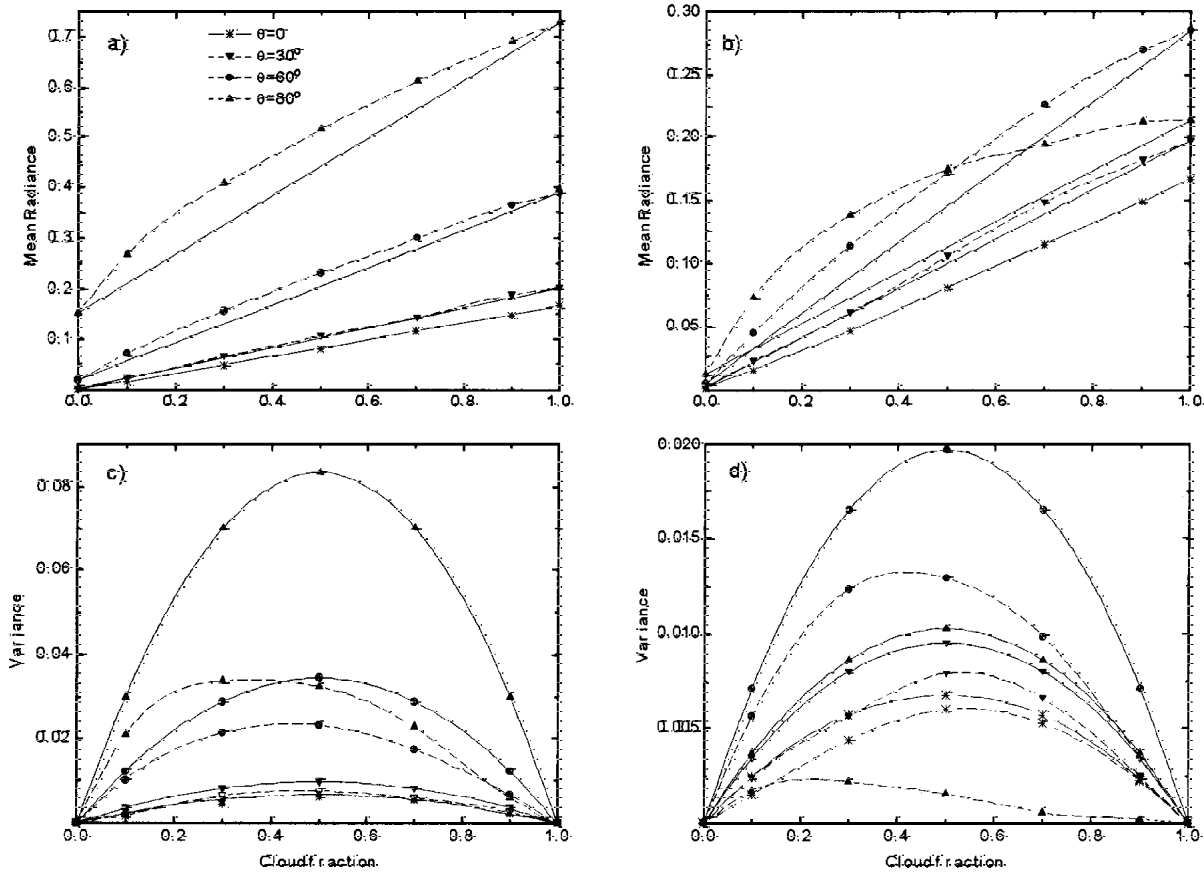
Figure 3. Dependencies of the mean (a, b) and variance (c, d) of intensity of reflected solar radiation on *N*, cloud fraction, with $\sigma = 30$ km^{-1}, $H = 0.5$ km, $D = 0.5$ km, $A_s = 0$ and for different zenith and azimuthal viewing angles; (a, c) $\varphi = 0°$, (b, d) $\varphi = 180°$. Here and in the following figures, $\xi_\otimes = 60°$, solid lines refer to stratus clouds, dashed lines indicate cumulus.

radiation reflected by the system "atmosphere-surface." From simple geometric considerations, it is clear that this contribution will be most significant for a range of viewing angles closest to zenith. This range will widen with the decrease of cloud fraction and with the increase of horizontal cloud sizes because both of these effects lead to the growth, on the average, of the solid angle at which a cloud gap ("hole") is seen from the ground. The results illustrated in Figure 4 are in accord with the aforesaid. Indeed, at $\varphi = 0°$, as A_s increases from 0.0 to 0.9, the mean intensity $£I_{Cu}ß$ in the direction $\theta = 30°$ increases nearly twofold, whereas for $\theta = 80°$, this growth is reduced to ~10%. At $\varphi = 180°$ and

for all θ values, $£I_{St}ß$ depends on A_s more strongly than does $£I_{Cu}ß$. Obviously, the contribution of radiation reflected from the surface *n* times will be proportional to the quantity

$$A_s^n \bullet \overline{Q} \bullet \overline{A}_d^{n-1} \tag{1}$$

where $\overline{Q}$ is the mean transmission of total solar radiation at the surface level (prior to reflection); and $\overline{A}_d$ is the albedo of the atmosphere, provided that its bottom is

illuminated by the diffuse radiation flux reflected from the surface. Since $\overline{Q}$ and $\overline{A}_d$ are cloud-type dependent, the underlying surface will contribute differently to the brightness field, depending on whether it is in cumulus or in equivalent stratus cloud system. It is obvious from Equation (1) that this contribution will sharply decrease with increasing multiplicity of reflection n, and that the dependence of the radiative statistical characteristics on surface albedo will be almost linear (Figure 4). For these reasons, qualitatively the radiative field will not reveal any strong dependence on surface albedo and hereafter we restrict ourselves to the $A_s = 0$ case. Radiation reflected from the surface somewhat smooths out the brightness contrast between the clouds and gaps ("holes"), so that the variance decreases with increasing A_s.

As σ, the extinction coefficient, grows from 15 to 120 km^{-1}, the mean intensities $\pounds I_{Cu}\ss$ and $\pounds I_{St}\ss$ increase by nearly a factor of 1.5 to 2.0 (Figure 5), a fairly clear and well-known result. In another way, the same result can be obtained by increasing the cloud fraction by ~0.1 - 0.2 (Figure 3). That is, the variations of cloud fraction are more important to the mean intensities than the variations in extinction coefficient. Increasing the extinction coefficient increases the difference between solar reflected intensities coming from clouds and those from cloud gaps, so that the intensity variance grows for both cumulus and stratus clouds.

At present, many statistics about the cloud microstructure have been accumulated. Cloud particle size distribution changes with season, geographic location, and cloud shape; in addition, it can alter significantly within a cloud.
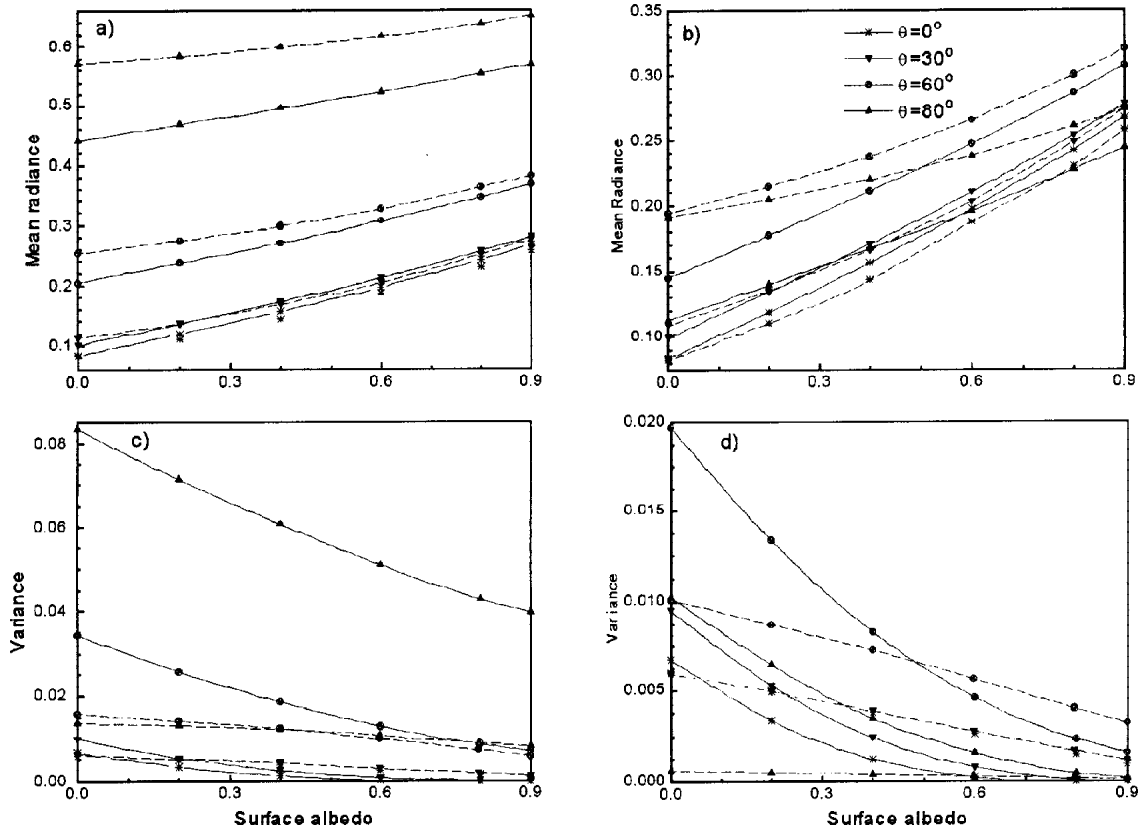

Figure 4. Influence of A_s, underlying surface albedo, on the mean (a, b) and variance (c, d) of intensity of reflected solar radiation with $N = 0.5$, $\sigma = 30\ km^{-1}$, $H = 0.5\ km$, $D = 0.25\ km$ and for different zenith and azimuthal viewing angles: (a, c) $\varphi = 0°$, (b, d) $\varphi = 180°$.
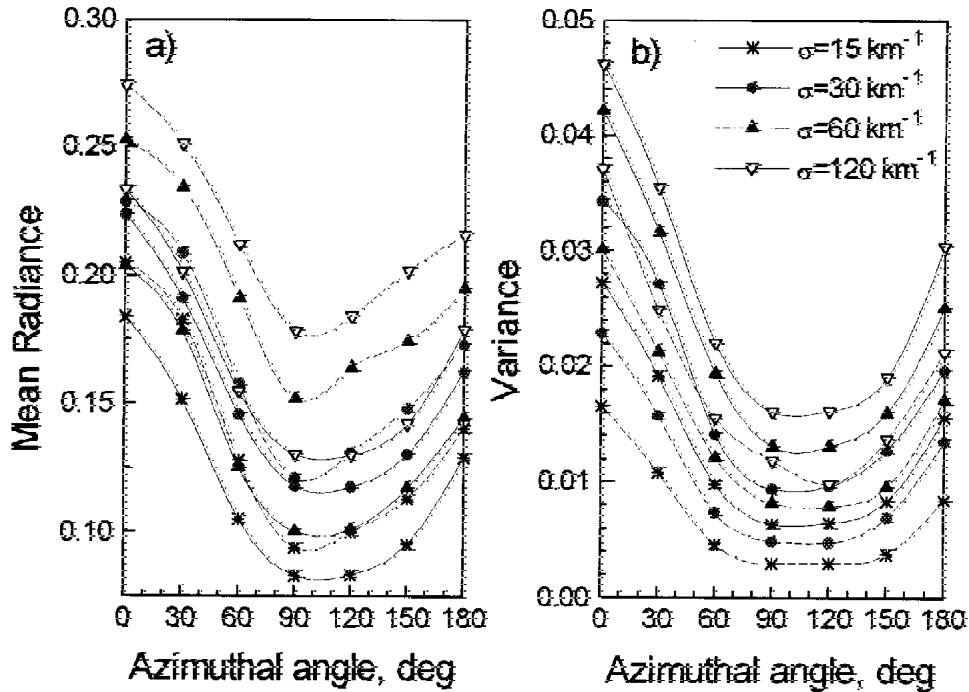
Figure 5. Dependence of the mean (a) and variance (b) of intensity of reflected solar radiation on azimuthal viewing angle, with $N = 0.5$, $H = 0.5$ *km*, $D = 0.5$ *km*, $A_s = 0$, $\theta = 60°$, and for different values of the extinction coefficient.

Because the droplet size spectrum depends on many factors, the construction of a cloud model is a rather complicated problem. In practice, several cloud models, differing not only in the parameters employed but also in the shape of the size distribution function of cloud droplets, are available for solving many important applied problems. In this regard, the question arises: How strongly does the choice of the model affect the radiative characteristics of broken and stratus clouds?

In our work, we have used three cloud models differing in the parameters of modified gamma distribution $n(r)$. The model parameters are listed in Table 1; here r_{eq} and r_{mean} are equivalent and mean radii, N_0, and w are the mean values of droplet concentration and water content, respectively. The C_1 and C_2 cloud models were taken from Deirmendjian (1969), while the C_6 model is from Welch et al. (1980).

Now we proceed to the analysis of cloud optical characteristics that are known to be determined by the

cloud microstructure. In the visible range, the extinction coefficient σ is related to r_{eq} by the expression (Kondratyev and Binenko 1984)

$$\sigma = \frac{3}{2}\frac{w}{\rho \bullet r_{eq}} \tag{2}$$

where ρ is the density of water in g/m^3 and

$$r_{eq} = \int_0^\infty n(r)r^3dr \bigg/ \int_0^\infty n(r)r^2dr \tag{3}$$

As seen from Equation (3) and Table 1, at a fixed water content, the extinction coefficient for the set of cloud models differs by more than a factor of twenty. Also, the scattering phase functions, as computed from the Mie theory at a wavelength of 0.69 μm, differ significantly.

Table 1. The parameters of modified gamma-distribution, $n(r)$.

Cloud Model	a	α	γ	r_m, μm	r_{eq}, μm	r_{mean}, μm	N_0, cm^{-3}	w, g/m^3
C_1	2.373	6	1	4	6.0	4.7	100	0.0625
C_3	5.5556	8	3	2	2.2	2.0	100	0.00377
C_6	0.0005	2	1	20	49.4	29.1	1.0	0.251

Particularly, at a zero scattering angle, the values of scattering phase functions can differ by more than two orders of magnitude.

Evaluate first the influence of the scattering phase functions (with the extinction coefficient and, hence, optical thickness fixed) on the brightness field of reflected solar radiation. As the scattering phase function becomes increasingly peaked forward, the mean intensity increases at large zenith viewing angles θ and decreases for viewing directions close to nadir (Figure 6). With given problem parameters, multiple scattering is unable to smooth the phase function-induced effects completely, so that the intensity mean and variance are markedly sensitive to the phase function variations for both cumulus and stratus clouds.

With the water content fixed, changes in the specific intensity are attributed to the variations in the scattering phase function and in the extinction coefficient (optical thickness). A significant decrease (by more than a factor of twenty) of optical cloud thickness, due to growing r_{eq}, leads to a considerable decrease of the mean intensity of reflected solar radiation (Figure 7). Clearly, the neglect of the cloud microphysical properties can lead to significant misestimates of the statistical characteristics of reflected solar radiation intensity that should be kept in mind, e.g., in interpretations of satellite data on the radiation budget of cloud fields. In view of the fact that the radiation fluxes are functions of the mean intensity, the GCM parameterizations of cloud radiative properties must include as basic parameters not only cloud fraction and water content, but also characteristic cloud droplet size. Note that large particle clouds (with particle radii > 40 - 50 μm) are able to reduce considerably the amount of reflected solar radiation both in the visible and near-IR spectral range (Wiscombe et al. 1984). Decreasing the mean optical thickness and

forward-elongating the scattering phase function (i.e., passing from C_3 to C_6 cloud model) enhances the transmission of cloudy layer and, thus, increases the contributions of undercloud, most optically dense aerosol and surface to formation of brightness field of reflected solar radiation. Because, with the given problem parameters, the under-cloud aerosol layer contributes to the mean reflected intensity nearly as strongly as do the stratus and cumulus clouds, in the C_6 model, the intensity variances will be nearly zero.

Summary

Algorithms of the Monte Carlo method are developed to calculate the mathematical expectation and variance of specific intensity of reflected solar radiation in a three-layer cloudy-aerosol atmosphere located over a lambertianly reflecting underlying surface. The algorithms are notable for their ability to calculate the mathematical expectation and variance of intensity in a given viewing direction, thus capturing rather fine features in the angular structure of reflected light.

Investigated are the mathematical expectation and variance of intensity of reflected solar radiation, modulated by cumulus and equivalent stratus clouds, as functions of cloud optical parameters, solar zenith angle, and surface albedo. The equivalence is taken to mean that the above indicated cloud types differ only in the mean horizontal size. It is shown that the effects associated with random geometry of cloud fields may lead to considerable qualitative and quantitative differences in mathematical expectation and variance of intensity between the cumulus and stratus clouds.
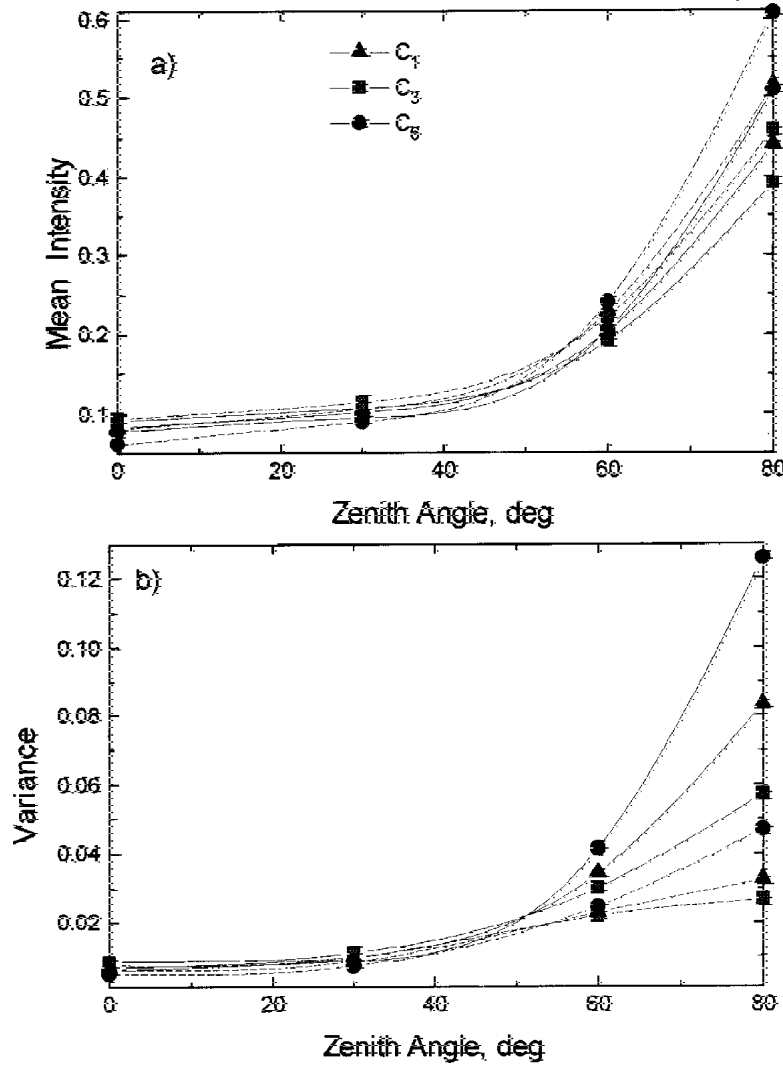
Figure 6. Dependence of the mean (a) and variance (b) of intensity of reflected solar radiation on zenith viewing angle, for scattering phase functions corresponding to the C_1, C_3, and C_6 cloud models, with $N = 0.5$, $\sigma = 30$ km^{-1}, $H = 0.5$ km, $D = 0.5$ km, $A_s = 0$, $\varphi = 0^\circ$.
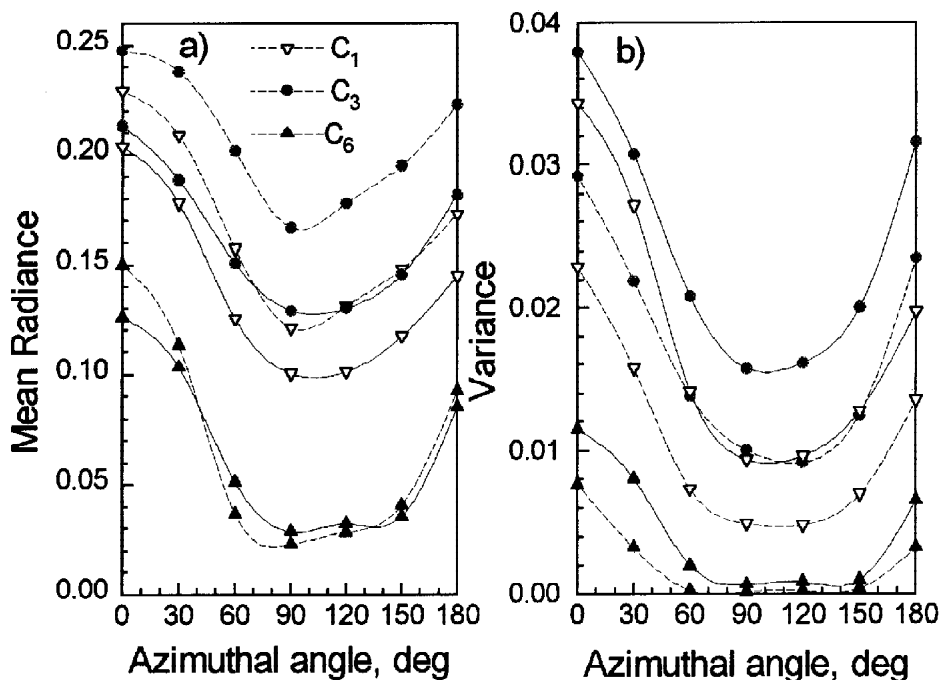
Figure 7. Dependence of the mean (a) and variance (b) of intensity of reflected solar radiation on azimuthal viewing angle, for water content fixed at $w = 0.12$ g/m^3, with $N = 0.5$, $H = 0.5$ km, $D = 0.5$ km, $A_s = 0$, $\theta = 60°$ and for different parameters of modified gamma distribution.

Acknowledgment

References

Atmosphere Handbook, ed. Sedunov Yu. S. et al. 1991. Leningrad, Gidrometeoizdat.

Barker, H. W., and J. A. Davies. 1992. Solar radiative fluxes for stochastic, scale-invariant broken cloud field. *J. Atmos. Sci.* **49**:1115-1126.

Davis, A., P. Gabriel, S. Lovejoy, D. Schertzer, and G. L. Austin. 1990. Discrete angle radiative transfer. Part III: Numerical results and atmospheric applications. *J. Geophys. Res.* **95**:11729-11742.

Davis, A. B., S. Lovejoy, and D. Schertzer. 1991a. Radiative transfer in multifractal clouds, pp. 303-318. *Scaling, Fractals and Non-Linear Variability in Geophysics*, eds., D. Schertzer and S. Lovejoy. Kluwer, Hingham, Massachusetts.

Davis, A. B., S. Lovejoy, and D. Schertzer. 1991b. Discrete angle radiative transfer in a multifractal medium. *S.P.I.E. Proceedings* **1558**:37-59.

Deirmendjian, D. 1969. *Electromagnetic Scattering on Spherical Polydispersions*. Elsevier.

Gabriel, P., S. Lovejoy, D. Schertzer, and G. L. Austin. 1988. Multifractal analysis of resolution dependence in satellite imagery. *Geophys. Res. Lett.* **15**:1373-1376.

Gabriel, P., S. Lovejoy, A. B. Davis, D. Schertzer, and G. L. Austin. 1990. Discrete angle radiative transfer-Part II: Renormalization approach for homogeneous and fractal clouds. *J. Geophys. Res.* **95**:11717-11728.

Green, R.N. 1980. The effect of directional radiation models on the interpretation of earth radiation budget measurements. *J. Atmos. Sci.* **37**:2298-2313.

Handbook of Clouds and Cloudy Atmosphere, ed., I. P. Mazin and A. K. Khragian. 1989. Leningrad, Gidrometeoizdat.

King, M. D., and R. J. Curran. 1980. The effect of a nonuniform planetary albedo on the interpretation of Earth radiation budget observation. *J. Atmos. Sci.* **37**:1262-1278,

King, M. D. 1987. Determination of the scaled optical thickness of clouds from reflected solar radiation measurements. *J. Atmos. Sci.* **44**:1734-1751.

Kondratyev, K. Ya., and V. I. Binenko. 1984. *Influence of Clouds on Radiation and Climate*. Leningrad, Gidrometeoizdat.

Pomraning, G. C. 1991a. *Linear Kinetic Theory and Particle Transport in Stochastic Mixtures*. World Scientific Publishing, Singapore.

Pomraning, G. C. 1991b. A model for interface intensities in stochastic particle transport. *J. Quant. Spectrosc. Radiat. Transfer* **46**:221-235.

Stephens, G. L. 1988a. Radiative transfer through arbitrarily shaped optical media. I: A general method of solution. *J. Atmos. Sci.* **45**:1818-1836.

Stephens, G. L. 1988b. Radiative transfer through arbitrarily shaped optical media. II: Group theory and simple closures. *J. Atmos. Sci.* **45**:1837-1848.

Titov, G. A. 1985. Radiative transfer in the broken cloudiness model constructed based on a Poisson point flux. *IZV. Acad. Sci., USSR Atmos. Oceanic Phys.* **21**:940-948.

Titov, G. A. 1987. Sensitivity of the mean radiant fluxes to the variations in the parameters of broken clouds. *IZV. Acad. Sci., USSR Atmos. Oceanic Phys.* **23**:851-858.

Titov, G. A. 1990. Statistical description of radiative transfer in clouds. *J. Atmos. Sci.* **47**:24-38.

Welch, R. M., S. K. Cox, and J. M. Davis. 1980. AMS Met. Monogr., **39**. American Meteorological Society, Boston, Massachusetts.

Wiscombe, W. J., R. M. Welch, and W. D. Hall. 1984. The effect of very large drops on cloud absorption. I: Parcel models. *J. Atmos. Sci.* **41**:1336-1355.

Yi, H. C., N. J. McCormick, and R. Sanchez. 1990. Cloud optical thickness estimation from irradiance measurements. *J. Atmos. Sci.* **47**:2567-2579.

Zhuravleva, T. B., and G. A. Titov. 1987. Angular distributions of solar radiation in broken clouds. *IZV. Acad. Sci., USSR Atmos. Oceanic Phys.* **23**:733-741.

Zhuravleva, T. B., and G. A. Titov. 1989a. Correlation of solar radiation intensity in broken cloudiness. *Issled. Zemli iz Kosmosa* No.4:35-43.

Zhuravleva, T. B., and G. A. Titov. 1989b. Statistical characteristics of outgoing short-wave radiation. *Issled. Zemli iz Kosmosa* No. 5:81-87.